High-temperature dolomite in the Lower Cretaceous Cupido Formation, Bustamante Canyon, northeast Mexico: petrologic, geochemical and microthermometric constraints

Gabriela Sara Guzzy-Arredondo[1,*], Gustavo Murillo-Muñetón[2], Dante Jaime Morán-Zenteno[3], José Manuel Grajales-Nishimura[2], Ricardo Martínez-Ibarra[2], and Peter Schaaf[3]

[1] Posgrado en Ciencias de la Tierra, Instituto de Geología, Universidad Nacional Autónoma de México, Ciudad Universitaria, 04510 México, D. F., Mexico.
[2] Instituto Mexicano del Petróleo, Programa de Investigación en Exploración Petrolera Eje Central Lázaro Cárdenas 152, 07730 México, D. F., Mexico.
[3] Instituto de Geología, Universidad Nacional Autónoma de México, Ciudad Universitaria, 04510 México, D. F., Mexico.
** gguzzy@servidor.unam.mx*

ABSTRACT

The Lower Cretaceous Cupido Formation, a carbonate system developed in northeastern Mexico, like many ancient carbonate platforms contains numerous dolomite bodies. These diagenetic features are particularly well exposed at Bustamante Canyon (Nuevo Leon State) where the Cupido Formation crops out from base to top along 6 km. Dolomitization affected practically all facies and crosscuts bedding planes; dolomite bodies are irregular in outer and margin platform facies and tabular/subhorizontal in inner platform facies. Most dolomite is replacive and also occurs as cement in small amounts. Crystal shape of replacement dolomite varies from nonplanar, planar-s to planar-e, whereas the dolomite cement consists mostly of saddle dolomite. Dolomite is non ferroan and shows dull red luminescence, its $\delta^{18}O_{PDB}$ *varies from -4.2 to -6.4‰ and its* $\delta^{13}C_{PDB}$ *from 1.8 to 3.4‰.* $^{87}Sr/^{86}Sr$ *ratios of replacement dolomite vary from 0.70754 to 0.70770. Homogenization temperatures in dolomite from fluid inclusion analysis range from 190 ºC to 200 ºC and are interpreted as the minimum temperatures for the dolomite formation. Petrographic data, geometries and distribution of dolomite bodies, microthermometric results from fluid inclusions and geochemical information suggest that the dolomitization occurred under deep-burial diagenetic conditions. Similar homogenization temperatures were determined in dolomite and post-dolomite calcite cement of the Cupido Formation from southern locations including Potrero Chico and Potrero Minas Viejas. The high temperatures recorded in the Cupido Formation dolomites are the result of a regional thermal anomaly developed probably around salt structures.* $^{87}Sr/^{86}Sr$ *values, oxygen stable isotopes, and trace element composition of dolomite suggest that the dolomitizing fluid was perhaps a hot mixture of formation water (modified sea water) of the Cupido Formation and brines derived from the updip La Virgen Formation, a carbonate-evaporite succession equivalent in age to the Cupido Formation. Dolomite distribution was apparently not controlled by major tectonic features (e.g., faults or fractures); the dolomitizing fluid seems to have followed subhorizontal or lateral flowing circulating patterns controlled by the former porosity and permeability of the calcareous facies.*

Key words: dolomite, high-temperature, thermal anomaly, Cupido Formation, Lower Cretaceous.

RESUMEN

La Formación Cupido del Cretácico Inferior, un sistema carbonatado desarrollado en el noreste de México, como muchas de las plataformas carbonatadas antiguas contiene numerosos cuerpos de

dolomita. Estas rasgos diagenéticos están particularmente bien expuestas en el Cañón de Bustamante (Estado de Nuevo León), donde la Formación Cupido aflora desde su base hasta su cima a lo largo de 6 km. La dolomitización afectó prácticamente todas las facies cruzando los planos de estratificación; los cuerpos de dolomita son irregulares en las facies de plataforma externa y margen de plataforma y tabulares a subhorizontales en las facies de interior de plataforma. La mayoría de la dolomita es de reemplazamiento y también ocurre como cemento en cantidades menores. Las formas de los cristales de la dolomita de reemplazamiento varían de no-planar, a planar-s y a planar-e; la dolomita de cemento es en su mayoría dolomita barroca. La dolomita es no ferrosa y exhibe luminiscencia opaca de color rojo, su $\delta^{18}O_{PDB}$ *varía de -4.2 a -6.4‰ y su* $\delta^{13}C_{PDB}$ *de 1.8 a 3.4‰. La relación* $^{87}Sr/^{86}Sr$ *de la dolomita de reemplazamiento varía de 0.70754 a 0.70770. Las temperaturas de homogeneización de la dolomita medidas en inclusiones fluidas varían de 190 a 200 °C y se interpretan como las temperaturas mínimas de formación de la dolomita. Los datos petrográficos, la geometría y la distribución de los cuerpos de dolomita, los resultados microtermométricos de inclusiones fluidas y la información geoquímica sugieren que la dolomitización ocurrió bajo condiciones diagenéticas de sepultamiento profundo. Temperaturas de homogeneización similares fueron determinadas en dolomita y cemento de calcita post-dolomita de la Formación Cupido de localidades más al sur, incluyendo Potrero Chico y Potrero Minas Viejas. Las altas temperaturas registradas en las dolomitas de la Formación Cupido son el resultado de una anomalía térmica regional desarrollada probablemente alrededor de estructuras salinas. Las relaciones de* $^{87}Sr/^{86}Sr$*, los isótopos de oxígeno y la composición de los elementos traza de la dolomita sugieren que el fluido dolomitizante fue posiblemente una mezcla caliente de agua de formación (agua marina modificada) de la Formación Cupido y salmueras derivadas de la Formación La Virgen, una sucesión carbonatada-evaporítica equivalente en edad a la Formación Cupido. La distribución de la dolomita no estuvo aparentemente controlada por rasgos tectónicos mayores (e.g., fallas o fracturas); los fluidos dolomitizantes parecen haber seguido patrones de circulación de flujo subhorizontal o lateral, controlados por la porosidad y permeabilidad originales de las facies calcáreas.*

Palabras clave: Dolomita, alta temperatura, anomalía térmica, Formación Cupido, Cretácico Inferior.

INTRODUCTION

The Cupido Formation is part of an extensive carbonate platform developed during Early Cretaceous time from northeastern Mexico to western Florida. This carbonate platform is exceptionally well exposed across northern Mexico, which allows conducting geologic research in great detail (Murillo-Muñetón, 1999). The age of the Cupido Formation ranges from upper Hauterivian to lower Aptian (Humphrey, 1949; Humphrey and Díaz, 1956; Guzmán, 1974; Alfonso-Zwanziger, 1978; Zárate-Mendoza, 1984; García *et al.*, 1989; McFarlan and Menes, 1991; Guzmán-García, 1991). This lithostratigraphic unit includes carbonate facies ranging from shallow water (inner platform and platform margin) to deeper water (outer platform) environments (Conklin and Moore, 1977; Selvius and Wilson, 1985; Murillo-Muñetón, 1999).

The diagenetic history of the Cupido Formation is poorly known. Only a few studies have been conducted to understand the diagenetic changes in the Cupido carbonate platform. Based on detailed petrography, Guzmán (1974) identified effects of marine, meteoric and burial diagenesis on the inner platform facies of the Cupido Formation at the Cortinas Canyon, State of Nuevo León. In their classic paper on the definition of saddle dolomite, Radke and Mathis (1980) included dolomite samples of the Sligo Formation which is the equivalent of the Cupido Formation in the United States Gulf Coast region. Moldovanyi and Lohmann

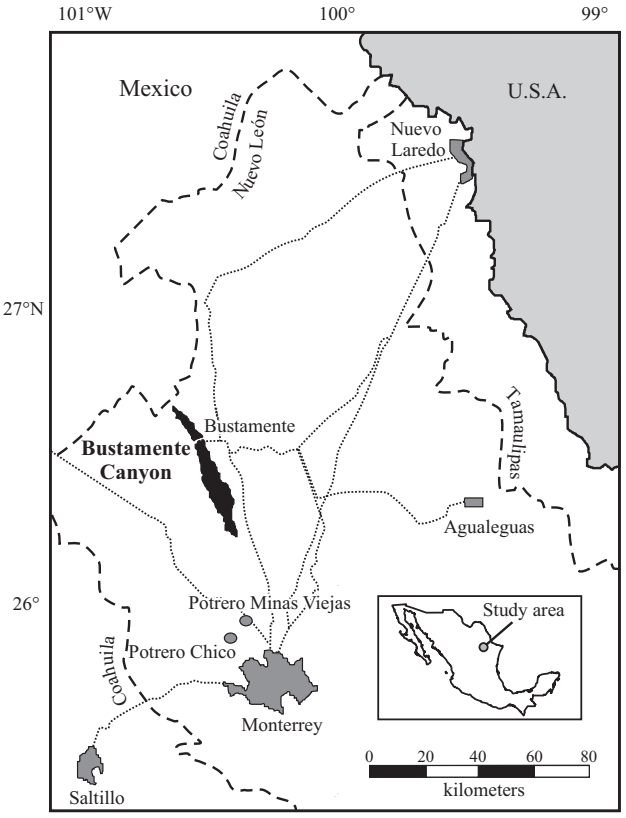

Figure 1. Location map of the Bustamante canyon, State of Nuevo León. The location of Potrero Minas Viejas and Potrero Chico is also shown.

(1984) estimated a $\delta^{18}O_{PDB}$ value of -2.0‰ and a $\delta^{13}C_{PDB}$ of +4.0‰ for the original marine carbonate composition for Lower Cretaceous time utilizing carbonate constituents of the Cupido and Sligo formations. Like most ancient carbonate systems, the Cupido platform commonly shows dolomitized segments, which are well exposed in northeastern Mexico. Bustamante Canyon is an extraordinary location where the Cupido Formation crops out completely from base to top; and the geometry of the dolomitized bodies can be traced accurately in two dimensions (Murillo-Muñetón, 1999; Murillo-Muñetón and Dorobek, 2003; Figures 1 and 2). Distribution and geometries of the dolomitized bodies of the Cupido Formation were mapped at Bustamante Canyon by Murillo-Muñetón (1999), who inferred that they could have been the result of deep-burial diagenesis conditions. However, a systematic study of the origin of these dolomite bodies was still lacking. Understanding the diagenetic processes, including dolomitization that affected the evolution of the porosity in the Cupido Formation, can be useful in oil exploration and production activities in the Sabinas Basin.

This paper presents the results of an integrated study of the dolomitization processes that affected the Cupido Formation exposed at Bustamante Canyon. The occurrence of high-temperature dolomite in the Cupido Formation is reported for the first time at this location, and its possible origin is discussed.

METHODS

To conduct this research, an integrated approach was followed to understand the dolomitization processes of the Cupido Formation at Bustamante Canyon. Several techniques were applied including: field work, petrography (plane light, cathodoluminescence and epifluorescence), major and trace element geochemistry, carbon and oxygen stable isotope analysis, strontium isotope analysis, and fluid inclusion thermometry.

Field work

A representative stratigraphic section on the northern wall of Bustamante Canyon was selected for this study on the basis of previous field work by Murillo-Muñetón (1999). This stratigraphic section was chosen where all the sedimentary facies of the Cupido Formation, including cyclic inner platform, platform margin and outer platform facies have been partially dolomitized. Reconnaissance work was also done to verify whether the underlying Taraises Formation and overlying La Peña Formation were affected by the dolomitization processes. Dolomite characteristics such as crystal shape and size according to the precursor limestone facies were recorded carefully. Forty two rock samples were collected and 85 additional

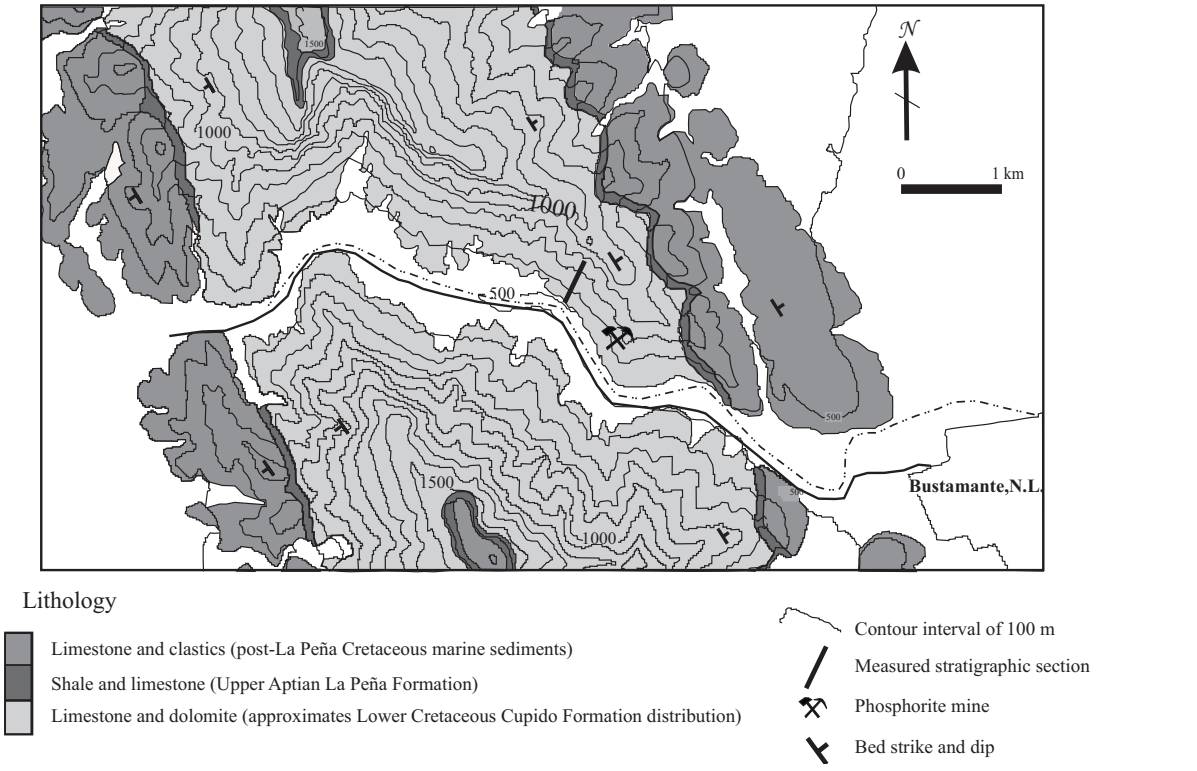

Figure 2. Geologic map of the Bustamante canyon, State of Nuevo León. The location of the representative stratigraphic section of the Lower Cretaceous Cupido Formation studied in this work is shown as a thick solid line in the northern wall of the canyon. Modified from Murillo-Muñetón and Dorobek (2003).

rock samples collected by Murillo-Muñetón (1999) were utilized for further petrographic, geochemical and thermometric analyses.

Petrography

One hundred and twenty seven thin sections were prepared for petrographic studies. The thin sections were stained with Alizarine Red S and K-ferricyanide following the technique of Dickson (1966). Depositional texture, grain constituents, cement types, and other major diagenetic features were documented for each sedimentary lithofacies. Dolomite characteristics such as crystal shape and size, presence of fluid inclusions and its timing relative to other diagenetic features (*e.g.*, compaction and stylolites) were carefully documented.

Cathodoluminescence petrography

A subset of 60 thin sections was chosen from the different dolomitized facies and was examined by cathodoluminescence. This work was done using a Relion luminoscope at the Instituto de Geología (Universidad Nacional Autónoma de México) and a Relion luminoscope coupled to a Nikon petrographic microscope with image analysis software at the Instituto Mexicano del Petróleo. Operating conditions in both places were: accelerating potential 15 kV, 250 μA beam current, and 0.01 torr for vacuum. Luminescence of replacement dolomite and dolomite cement as well as post-dolomite calcite cement was recorded. Special attention was focused on the presence or absence of luminescence zoning in the diagenetic mineral phases.

Geochemical analyses

Field relationships and the results from plane light/cathodoluminescence petrography were used to select representative samples of dolomite from the different facies for geochemical studies. These analysis included major and trace element geochemistry, oxygen and carbon stable isotope geochemistry and strontium isotopes.

Major and trace element geochemistry

Six samples of dolomite and one of post-dolomite calcite cement were analyzed for major and trace element composition. A total of 84 points (analyses) were examined utilizing a Cameca electron microprobe at the Texas A&M University (Department of Geology and Geophysics, College Station, Texas). Operating conditions were as follows: accelerating voltage 15 kV, beam current 15 nA, and beam diameter 10 μm. Major elements quantified included Ca and Mg; and trace elements included: Fe, Mn, Na, and Sr. Lower detection limits, in ppm, for trace element measurements were: 20, 100, 90, 130, and 30 for Mg, Fe, Mn, Sr, and Na, respectively.

Oxygen and carbon stable isotopes

Oxygen and carbon stable isotope analyses were performed on six samples of individual replacement dolomite, six samples of bulk dolomite, two samples of original marine calcite, and one sample of post-dolomite calcite cement at the Stable Isotope Laboratory of the Laboratorio Universitario de Geoquímica Isotópica (LUGIS) of the Instituto de Geología (Universidad Nacional Autónoma de México). The isotopic ratios represent bulk compositions of replacement dolomite and post-dolomite calcite cement. Rock samples were crushed in an agate mortar. Replacement dolomite was extracted by hand with pointed pliers and a dissection needle. Special care was taken to exclude dolomite cement from the analyses. The dolomite concentrates were cleaned with deionized water in an ultrasonic bath, dryed and powdered in an agate mortar. The original marine calcite was extracted also by hand utilizing a dissection needle and a microdrill. These samples were taken directly from a bivalve shell on a thin section under a petrographic microscope. All carbonate samples were placed in individual test tubes. They were washed with acetone in an ultrasonic bath for 30 minutes and dried in an oven at 80 ºC. Approximately 400 μg of powdered sample was employed for each isotopic analysis. Samples were reacted with orthophosphoric acid at 25 ºC for calcite and at 72 ºC for dolomite; the produced CO_2 gas was fed directly into the mass spectrometer. The isotopic ratios were measured in a Thermoquest Finnigan Delta Plus-XL mass spectrometer with dual inlet, Gas Bench II as interface utilizing an autosampler GC PAL. The isotope ratio was determined simultaneously for carbon and oxygen following the procedure described by Revez *et al.* (2001) and Revez and Landwehr (2002). Isotopic ratios were measured relative to the NBS-18 and LSVEC standards and converted to PDB values. Accuracy of the analyses was checked using a calcite reference sample which was analyzed every seven samples. The standard deviation reported is 0.2‰ for $\delta^{18}O$ and 0.2‰ for $\delta^{13}C$.

Strontium isotopes

The $^{87}Sr/^{86}Sr$ ratios of six samples of replacement dolomite, two samples of original marine calcite and one sample of post-dolomite calcite cement from the Cupido Formation were measured at LUGIS of the Instituto de Geofísica. Additionally, the $^{87}Sr/^{86}Sr$ ratios of two samples of gypsum, three samples of marine lime mud and three samples of fine-grained dolomite from the La Virgen Formation, an updip time-equivalent stratigraphic unit of the Cupido Formation, were measured. Sr-Spec resin (Eichcrom®) was used to separate strontium, nitric acid (8N) for sample dissolution, nitric acid (3N) for column cleaning, and milli Q water to collect the Sr. The isotopic ratios were measured in a Finnigan MAT 262 thermal ionization mass spectrom-

eter equipped with a variable multicollector system (eight Faraday cups) in static mode. The samples were loaded as chlorides on double rhenium filaments and were measured as metallic ions. Sixty Sr isotopic ratios (n) were measured for each sample. Reported analytical errors (1sd) are referred to the last two digits. The standard utilized was NBS 987 ($^{87}Sr/^{86}Sr = 0.710237 \pm 21$; n = 317). All Sr isotopic ratios were corrected for mass fractionation by normalizing to $^{87}Sr/^{86}Sr = 0.1194$. The average analytical blank obtained during the time of the sample analyses was 5.5 ng Sr (total blank). For interpretation of the $^{87}Sr/^{86}Sr$ ratios, the Burke's marine Sr isotope curve recently improved by McArthur *et al.* (2001) was utilized and the absolute values were referred to the International Stratigraphic Chart (International Commission of Stratigraphy, 2004).

Fluid inclusion microthermometry

Fluid inclusion microthermometry was carried out to estimate the crystallization homogenization temperatures of dolomites of the Cupido Formation. Ninety eight measurements of homogenization temperature (Th) were made on six dolomite samples. Thirty two measurements were made on three samples of post-dolomite calcite cement. These analyses were conducted at the Instituto Mexicano del Petróleo employing a Linkam heating-cooling stage (model THMSG-600) adapted to a petrographic microscope. The equipment also includes a monitor to observe phase changes that occur to the fluid inclusions; a computer allows the total control of the instrument performance. The stage is connected to both a temperature controller that heats up the sample and to a cooling pump that circulates liquid nitrogen. Temperature range varies from -180 ºC to 600 ºC with both devices. Heating velocity of the analyses was 10 ºC/min. The standard utilized for calibration was synthetic quartz; it was calibrated with H_2O at critical density (0 ºC and 374.1 ºC) and also calibrated with H_2O and CO_2 (25%M; -56.6 ºC). For this study, only primary fluid inclusions were considered, avoiding those fluid inclusions showing necking down. An additional group of seven samples were analyzed under epifluorescence in a petrographic microscope with an adapted mercury lamp to identify hydrocarbon fluid inclusions.

REGIONAL GEOLOGIC FRAMEWORK

Excellent outcrops of Mesozoic strata in northeast Mexico are distributed across the Coahuila Folded Belt and the Sierra Madre Oriental. The outcropping stratigraphy in this region includes marine sedimentary rocks that range in age from Middle Jurassic to early Tertiary. This heterogeneous sedimentary package is the result of the opening and subsequent evolution of the Gulf of Mexico Basin (Salvador, 1987; Wilson, 1990; Goldhammer *et al.*, 1991; Michalzik, 1991). The central parts of some localities (*e.g.*, Potrero Minas Viejas and Potrero Chico) contain Middle Jurassic marine evaporites (gypsum and halite) of the Minas Viejas Formation (Salvador, 1987; Wilson, 1990; Goldhammer *et al.*, 1991; Michalzik, 1991). Upper Jurassic carbonate-evaporitic strata of the Oxfordian Zuloaga Formation are the oldest marine carbonate sediments in the region and unconformably overlie Upper Triassic continental beds of the Huizachal or Boca Formation (Carrillo-Bravo, 1961). Marine carbonates, evaporites and terrigenous sediments of the Olvido and La Gloria formations (Kimmeridgian) as well as marine siliciclastic rocks of the La Casita Formation (Kimmeridgian-Berriasian) make up the remainder of the Upper Jurassic strata in this area.

The Lower Cretaceous stratigraphy in northeastern Mexico shows important vertical and lateral facies variations. These strata include both shallow-water and deep-water carbonates, inner platform evaporites, and continental and marine siliciclastic sediments. A thick section of fluvial and shallow-marine sediments was deposited adjacent to the Coahuila paleo-Peninsula during Berriasian-Hauterivian time. These include conglomerates, sandstones, shales, and limestones of the San Marcos Arkose, Patula Arkose, Menchaca, and Barril Viejo formations (Figure 3). These units grade basinward into coeval deeper-water marine shales and limestones of the Taraises Formation.

During late Hauterivian to early Aptian time, the Cupido carbonate system was developed in the region. Updip, limestones and shales of the La Mula Formation followed by cyclic carbonates and evaporites of the La Virgen Formation as well as shallow-water carbonates of the Cupido Formation were accumulated in inner platform region (Humphrey and Díaz, 1956; Guzmán-García, 1991; Hernández-Trejo, 2003). The Cupido platform margin facies tract consists of rudist fragment-rich grainstone and packstone with minor rudist boundstone. These facies change seaward to open marine lime mudstone and basinal carbonates of the Lower Tamaulipas Formation (Murillo-Muñetón, 1999, and references therein).

During the late Aptian, the Cupido carbonate platform was succeeded by open marine shaly carbonates of the La Peña Formation (Salvador, 1987; Wilson, 1990; Goldhammer *et al.*, 1991; McFarlan and Menes, 1991; Murillo-Muñetón, 1999). The middle and Upper Cretaceous is represented by deep-water carbonates (Upper Tamaulipas and Aurora formations) and shaly carbonates and siliciclastic facies (San Felipe and Mendez formations, Parras Shale and Difunta Group; Humphrey and Díaz, 1956; Weidie and Murray, 1967; Padilla y Sánchez, 1978; Wilson *et al.*, 1984).

Finally, during Late Cretaceous time, the tectonic regime changed dramatically from a typical passive margin regime to a compressional tectonic scenario as a consequence of the Laramide Orogeny that ended in Eocene time (Lawton and Giles, 1997). The Coahuila Folded Belt, the Sierra Madre Oriental, and the Parras and La Popa foreland

basins were formed during the Laramide Orogeny (Kellum *et al.*, 1936; Imlay, 1936; Humphrey and Díaz, 1956; Charleston, 1973, 1981).

STRATIGRAPHY AND SEDIMENTOLOGY OF THE CUPIDO FORMATION IN NORTHEASTERN MEXICO

As mentioned above, the Cupido Formation represents a marine carbonate platform that includes inner platform, platform margin and open marine facies. This carbonate system represents a large-scale prograding carbonate platform with lower hierarchy transgressive-regressive cycles developed from late Hauterivian to early Aptian time in a passive margin (Goldhammer *et al.*, 1991; Goldhammer, 1995, 1999; Lehmann *et al.*, 1998, 1999, 2000; Murillo-Muñetón, 1999). The Cupido platform has traditionally been considered as a rimmed shelf, however, extensive field work suggests that during its early development the platform had rather a low-angle, ramp-type depositional profile in the study area (Murillo-Muñetón, 1999; Murillo-Muñetón and Dorobek, 2003).

Sedimentary facies

A brief description of the Cupido Formation sedimentary facies at Bustamante Canyon is given in this section; for further details refer to Murillo-Muñetón (1999). Shallow-water subtidal facies constitute the inner platform and platform margin facies tracts. Interior platform facies are typically arranged cyclically, forming shallowing-upward subtidal cycles. A typical cycle begins with a highly bioturbated lime mudstone/wackestone or a skeletal-coated grain-peloidal packstone/grainstone that grades upward to a skeletal-coated grain-peloidal packstone/grainstone. Skeletal carbonate grains in the cycles include shallow-water marine biota such as fragments of rudists (mainly requieniids), green calcareous algae (dasycladacean and codiacean algae), red coralline algae, gastropods, corals, echinoderms, ostracodes, and benthic foraminifers. The platform margin facies consist of massive rudist fragment-peloidal-skeletal-intraclast packstone, and scarce buildups of coral-stromatoporoid-rudist boundstone. Cycles are apparently absent in the platform margin facies tract. Skeletal carbonate grains in this tract are similar to those in the inner platform facies but with a significant amount of fragments of caprinid and requieniid rudists.

Open platform facies include both outer ramp facies and deep ramp/basin facies. Outer ramp facies consist of medium- to thick-bedded, peloidal-skeletal-intraclast wackestone and packstone with chert nodules. Benthic foraminifers, ostracodes, and fragments of echinoderms, bryozoans, mollusks, as well as whole fossils of pelecypods, siliceous sponges, and small solitary and colonial corals comprise the skeletal content in these strata. Deep ramp/basin facies consist of lime mudstone and shaly lime

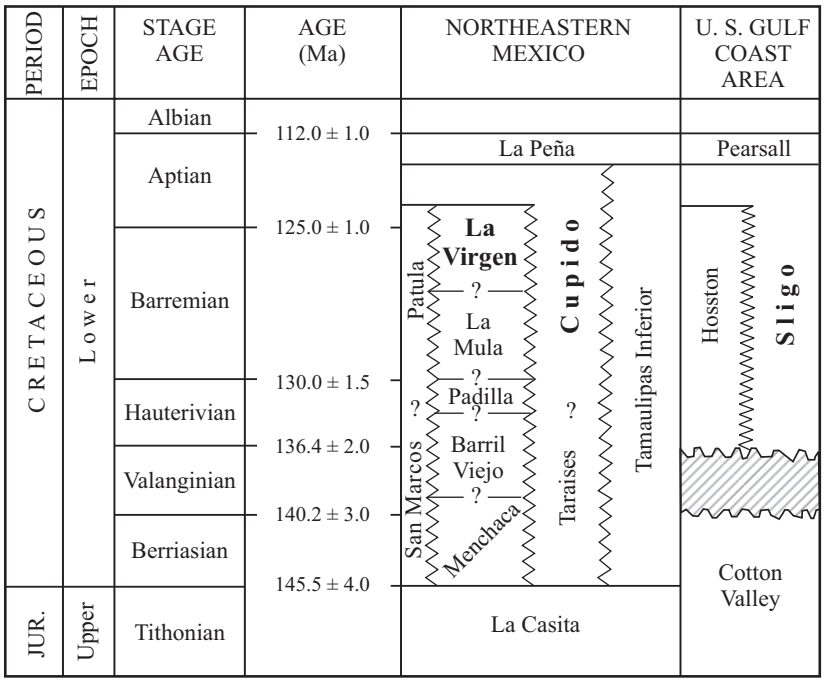

Figure 3. Lower Cretaceous stratigraphic chart of northeastern Mexico and the U.S. Gulf Coast area. Note the stratigraphic position of the Lower Cretaceous La Virgen Formation, which is an updip (inner platform) equivalent of the Cupido Formation and is mentioned in the text. Modified from Murillo-Muñetón (1999). Numerical ages after the International Stratigraphic Chart (International Commission on Stratigraphy, 2004).

mudstone. The lime mudstone facies are medium to very thick bedded and show bioturbation whereas the shaly lime mudstone facies are typically thin and nodular bedded. The skeletal content in these facies is poor and includes small benthic foraminifers, ostracodes, and fragments of bryozoans, echinoderms, mollusks, and siliceous sponges.

Numerous carbonate mud mounds also developed throughout the Cupido platform margin and outer platform settings at Bustamante Canyon. Further details on these organic carbonate buildups are presented in Murillo-Muñetón (1999) and Murillo-Muñetón and Dorobek (2003). Four types of carbonate mud mounds occur at this location: Type 1 siliceous sponge-microbial mud mounds; Type 2 sponge-microbial mud mounds; Type 3 sponge microbial-coral mud mounds; and Type 4 calcisponge-microbial-coral biodetrital mud mounds. Type 1 siliceous sponge-microbial mud mounds are the oldest and most abundant mounds; they grow up adjacent to deep ramp/basinal lime mudstone facies. These carbonate buildups consist of microbial mud with siliceous sponges and encrusting organisms such as bryozoans, foraminifers, and agglutinating and serpulid worm tubes. Type 2 sponge-microbial mud mounds are associated with outer ramp wackestone/packstone facies and their fossil content is similar to that of the sponge-microbial mud mounds, but they also contain calcareous sponges, red coralline algae and benthic foraminifers. Type 3 sponge-microbial-coral mounds developed adjacent to outer ramp packstone facies, and their skeletal components are similar to those of Type 2 mounds but also contain small colonial corals. Pockets of skeletal grains are common in mounds of types 2 and 3. Type 4 calcisponge-microbial-coral biodetrital mounds are the youngest mounds and are associated with outer ramp packstone and ramp crest rudist packstone facies. These carbonate buildups also contain abundant shallow-water skeletal constituents including benthic foraminifers, worm tubes, and fragments of calcareous algae, gastropods, pelecypods, and echinoderms. Both length and height of individual Type 1, 2, and 3 mounds range from a few to tens of meters whereas Type 4 mounds reach several hundred meters in length and are up to 90 m thick.

DISTRIBUTION AND CHARACTERIZATION OF THE CUPIDO FORMATION DOLOMITE AT BUSTAMANTE CANYON

Dolomite distribution and its controls at Bustamante Canyon

Dolomite bodies in the Cupido Formation show a complex but systematic distribution at Bustamante Canyon. The dolomite distribution was controlled, in part, by the type of sedimentary facies that was eventually dolomitized. Overall, two main geometries in the dolomite bodies are distinguished: (1) very irregular dolomite bodies and (2) tabular/subhorizontal dolomite bodies. The irregular dolomite bodies occur within the lower part of the Cupido Formation where the carbonate mud mounds are abundant. These dolomite bodies form large carbonate masses that are partially to completely dolomitized. Dolomitization in these bodies crosscuts bedding planes and is more penetrative in the facies containing the shallowest-water carbonate mud mounds (types 3 and 4) and less intense in the lime mud-rich facies containing the deeper-water carbonate mud mounds (types 2 and 1). In contrast, tabular/subhorizontal dolomite bodies occur in the upper part of the Cupido Formation consisting of lime mud-poor, cyclic inner platform facies. Dolomitization, often, was more pervasive in the lower transgressive part of the cycles. Since the Cupido Formation at this location is completely exposed from base to top, it is clear that the dolomite is distributed, to different degrees, throughout this lithostratigraphic unit. Nevertheless, the dolomitization event did not affected the sedimentary facies of both the underlying Taraises and overlying La Peña formations. Furthermore, it is also clear that the dolomite bodies are not spatially related to faulting. Although normal faults with a few meters of displacement occur at this location, no major faults that might have controlled the dolomite distribution are present at Bustamante Canyon (Murillo-Muñetón, 1999).

Dolomite types

Two main dolomite types can be distinguished petrographically in the Cupido Formation at Bustamante Canyon. The most abundant type is replacement dolomite and the less common is dolomite cement. Crystal size of the replacement dolomite was controlled, in part, by the depositional texture of the sedimentary facies that were subsequently dolomitized. Crystal size of dolomite varies from very fine to coarse-grained (30 μm to ~2 mm). Very-fine grained dolomite replaced calcareous mud, peloids, and calcite cement veins. Medium- and coarse-grained dolomite replaced blocky calcite cement and larger carbonate constituents including skeletal grains and intraclasts. Thus, fine-grained dolomite occurs mostly in carbonate mud-rich facies such as lime mudstone and wackestone lithofacies whereas coarser dolomite is found mostly in carbonate mud-poor lithofacies such as packstone and grainstone. Likewise, dolomitized deep-water carbonate mud mounds (types 1 and 2) contain commonly fine-grained dolomite whereas dolomitized shallower-water carbonate mud mounds (types 3 and 4) contain coarser-grained dolomite. Following the classification by Sibley and Gregg (1987), shapes of dolomite crystals in the Cupido Formation include: anhedral (nonplanar), subhedral (planar-s), and euhedral (planar-e) (Figure 4). The most abundant is nonplanar dolomite and the less common are planar-s and planar-e. Some dolomite crystals have cloudy cores, due to the presence of fluid inclusions, and limpid rims. Dolomite cement is found filling voids related to primary porosity, intercrystalline porosity and small frac-

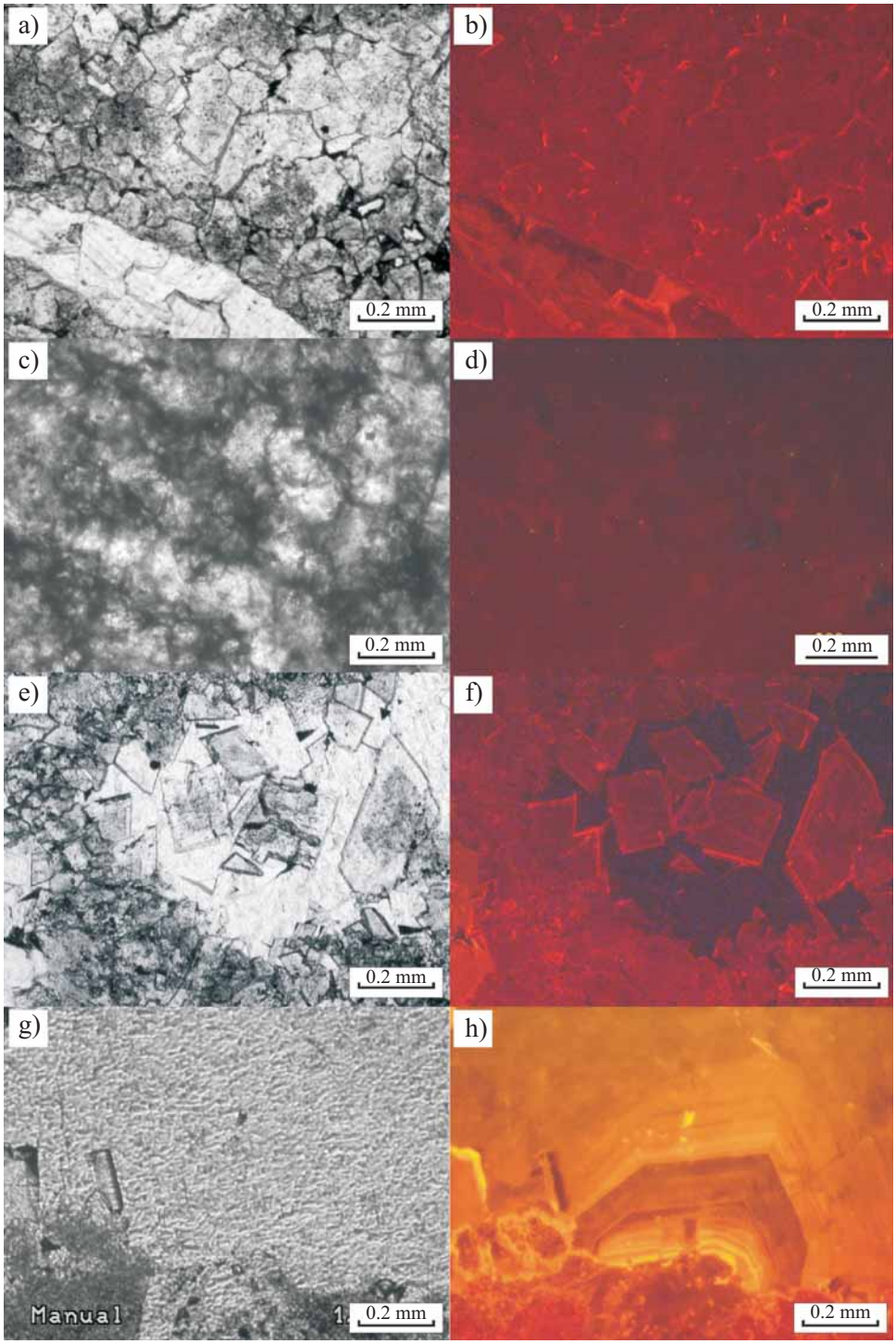

Figure 4. Paired plane-light and cathodoluminescence photomicrographs of the Cupido Formation diagenetic phases. a: Plane light photomicrograph of medium-grained planar-s replacement dolomite. b: Cathodoluminescence photomicrograph of (a); the replacement dolomite shows a homogeneous red dull color with no zoning. c: Plane light photomicrograph of fine- to medium-grained nonplanar replacement dolomite. d: Cathodoluminescence photomicrograph of (c), similar to (b), the replacement dolomite shows also a homogeneous red dull color lacking zoning. e: Plane light photomicrograph of a planar-s replacement dolomite and subhedral/euhedral dolomite cement with cloudy cores and limpid rims. f: Cathodoluminescence photomicrograph of (e), similar to (b) and (c), both the replacement dolomite and the dolomite cement are red dull luminescent with no zoning. g: Plane light photomicrograph of a vein of post-dolomite calcite cement. h: Cathodoluminescence photomicrograph of (g), in contrast to the dolomite crystals, this cement shows a bright orange color with well developed zoning.

tures resulting from deep-burial diagenetic events (Figure 4e). Dolomite cement is commonly euhedral and its size ranges from medium to coarse (0.1 mm a 2.3 mm; Figure 4e). Most dolomite cement has cloudy cores and limpid rims and some is saddle dolomite. Under epifluorescence petrography, some dolostone samples show a yellow color along the crystal boundaries due to the presence of aromatic hydrocarbons. Fluorescence is not observed inside dolomite crystals suggesting that the fluid inclusions lack liquid hydrocarbons. A common late diagenetic phase consists of post-dolomite blocky calcite cement that fills crystalline porosity and fractures (Figure 4h).

Cathodoluminescence petrography of dolomite

Cathodoluminescence patterns of carbonate constituents were analyzed in 60 representative samples of the Cupido Formation. Luminescence of the different components and diagenetic phases of the precursor limestones, dolostones and post-dolomite calcite cement was documented. Overall, the original carbonate phases of the limestones show no luminescence. Both replacement dolomite and dolomite cement show dull luminescence with a typical homogeneous red color lacking zoning (Figures 4b, 4d and 4f).). In contrast, the post-dolomite blocky calcite cement shows concentric zoning consisting of alternating brilliant bands, dull bands and non-luminescent bands (Figure 4h).

Geochemistry of dolomites

Major and trace elements

From major element analyses, the Ca/Mg ratio of the Cupido Formation replacement dolomite varies from 1.03 to 1.10 (Table 1). This ratio indicates that the replacement dolomite of the Cupido Formation is very close to stoichiometry (Scoffin, 1987; Morse and Mackenzie, 1990; Tucker and Wright, 1990). The trace element abundances in the dolomite from different dolomitized lithofacies and different stratigraphic position vary as follows: 111 to 3,292 ppm for Fe; 91 to 234 ppm for Mn; 30 to 566 ppm for Na; and 131 to 1,608 ppm for Sr. There is no obvious pattern in those variations between samples nor between cores and rims of individual dolomite crystals (Figure 5a and 5b). The post-dolomite calcite cement has the following trace element concentrations: 207 to 3,148 ppm for Fe; 91 to 235 ppm for Mn; 56 to 616 ppm for Na; and 134 to 789 ppm for Sr. Compared to the Fe content, Mn concentration is relatively low (91 to 234 ppm) in all samples.

Oxygen and carbon stable isotopes

The $\delta^{18}O_{PDB}$ values of the Cupido Formation replacement dolomites at Bustamante Canyon ranges from -6.4 to -4.2‰ (Figure 6; Table 1). Similar oxygen isotopic composition was determined from two primary marine constituents taken from rudist walls (-6.2 and -4.4‰, PDB). A $\delta^{18}O_{PDB}$ value of the post-dolomite calcite cement is remarkably ^{18}O-depleted (-10.2 $^{0}/_{00}$). Murillo-Muñetón and Dorobek (2003) reported the following oxygen isotopic compositions for marine constituents of the Cupido Formation mud mounds: -6.5 to -3‰ for carbonate components of Type 1, 2, and 3 mounds and -10 to -6.5‰ for carbonate components of Type 4 mounds. Furthermore, unpublished isotopic data by G. Murillo-Muñetón for Cupido Formation replacement dolomite (-6.9 to -5.1‰), and post-dolomite calcite cement (-12.2 to -7.2‰) are similar to the geochemical results obtained in this study. A pristine oxygen isotopic value for the Early Cretaceous marine water has not been established for the Cupido Formation limestones in northeastern Mexico (Murillo-Muñetón, 1999). However, a $\delta^{18}O_{PDB}$ value of -2.0‰ was estimated by Moldovanyi and Lohman (1984) to represent the original marine carbonate composition for Lower Cretaceous time utilizing marine calcium carbonate constituents mainly from the Sligo Formation, which is the equivalent to the Cupido Formation in the United States Gulf Coast area. Therefore, the oxygen isotopic composition of the different carbonate components in this work suggests a temperature-diagenetic effect that is discussed below.

The $\delta^{13}C_{PDB}$ values for the two samples of rudist walls are +0.5 and +2.5‰. The carbon isotopic composition of the Cupido Formation replacement dolomite ranges from +1.8 to +3.4‰ (PDB). Considering that the carbon isotopic marine values reported by Moldovanyi and Lohman (1984) for the Sligo/Cupido Formation marine carbonates vary from +1.8 to +4.0‰ (PDB), then the $\delta^{13}C_{PDB}$ values of the Cupido Formation carbonates (calcite and dolomite) reported in this work reflect a somewhat typical marine isotopic composition (Hudson, 1977; Lohmann, 1988; Tucker and Wright, 1990; Allan and Wiggins, 1993).

Strontium isotopes

The$^{87}Sr/^{86}Sr$ ratios of the Cupido Formation carbonate phases at Bustamante Canyon range from 0.70749 to 0.70770 (Table 1). The $^{87}Sr/^{86}Sr$ ratios of replacement dolomite vary from 0.70754 to 0.70770. The measured $^{87}Sr/^{86}Sr$ ratio for a sample from the precursor limestone was 0.70749 which is slightly lower but significantly different to those of the dolomites. A $^{87}Sr/^{86}Sr$ value of 0.70752 was determined for a sample of post-dolomite calcite cement. The $^{87}Sr/^{86}Sr$ ratio of the original limestone intersects the Burke's Sr-isotope curve improved by McArthur *et al.* (2001) at three different dates: 81.5 Ma(Campanian), 126 Ma (Barremian), and 197 Ma (Sinemurian). Since the age of the lower part of the Cupido Formation is upper Hauterivian to Barremian (Murillo-Muñetón, 1999), it is reasonable to interpret the $^{87}Sr/^{86}Sr$ value of 0.70749 from the precursor limestone most likely as the value of Barremian marine water (Table 1). On the other hand, the $^{87}Sr/^{86}Sr$ values for the replacement dolomites and post-dolomite calcite cement are higher than those of the late Hauterivian to early Aptian marine water (McArthur *et al.*, 2001), but are similar to

Table 1. Ca/Mg, and strontium isotopic ratios, carbon and oxygen isotopic composition, and fluid inclusion microthermometry of Cupido Formation carbonates from the Bustamante Canyon.

Stratigraphic position (m)	Sample	Mineral	Ca/Mg ratio	$^{87}Sr/^{86}Sr$	n	1 sd	Bulk dolomite		Replacement dolomite fractions		Calcite		Homogenization temperature* (°C)	Melting temperature (°C)	Remarks
							$\delta^{18}O_{PDB}$	$\delta^{13}C_{PDB}$	$\delta^{18}O_{PDB}$	$\delta^{13}C_{PDB}$	$\delta^{18}O_{PDB}$	$\delta^{13}C_{PDB}$			
383	BCA-70	Dolomite	1.03	0.70765	59	42	-5.7	2.7					190 to 200		Dolomitized shallow-water wackestone/packstone facies
346	BCA-65	Dolomite	1.04	0.70754	52	43	-5.4	3.1	-5.2	3.1			190 to 200		Dolomitized shallow-water mudstone/wackestone facies
305	BCA-60	Dolomite	1.03	0.70756	56	42	-6.4	1.8					190 to 200		Dolomitized shallow-water peloidal-skeletal wackestone/packstone facies
274	BCA-52	Dolomite	1.02	0.70770	55	41	-5.2	3.0	-5.4	3.0			190 to 200		Dolomitized shallow-water peloidal-skeletal packstone/grainstone facies
239	BCA-46	Calcite (rudist wall)		0.70749	53	41					-6.2	0.5			Shallow-water rudist-peloidal-skeletal-lithoclastic packstone facies
154	BCA-32	Dolomite	1.03	0.70758	57	41	-4.8	2.9	-4.2	3.2			190 to 200		Dolomitized calcisponge-microbial-coral biodetrital mud mound
116	BCA-VX	Dolomite Post-dolomite calcite	1.04	0.70752	59	39					-10.2	-5.2	190 to 200 138 to 220	-20.3, -8, and -3.7	Dolomitized deeper-water peloidal-skeletal packstone facies. -20.3= 22.6 wt.% NaCl; -8 =11.7 wt.% NaCl; and -3.7= 6 wt.% NaCl.
60	BCA-18	Dolomite Post-dolomite Calcite	1.10	0.70759	53	42	-4.6	3.4	-5.0	3.3			190 to 200 138 to 220		Dolomitized deeper-water siliceous sponge-microbial mud mound

Younger samples →

* Thermometric data represent the range of homogenization temperature. n = number of individual isotopic determinations; 1 sd = 1 standard deviation.

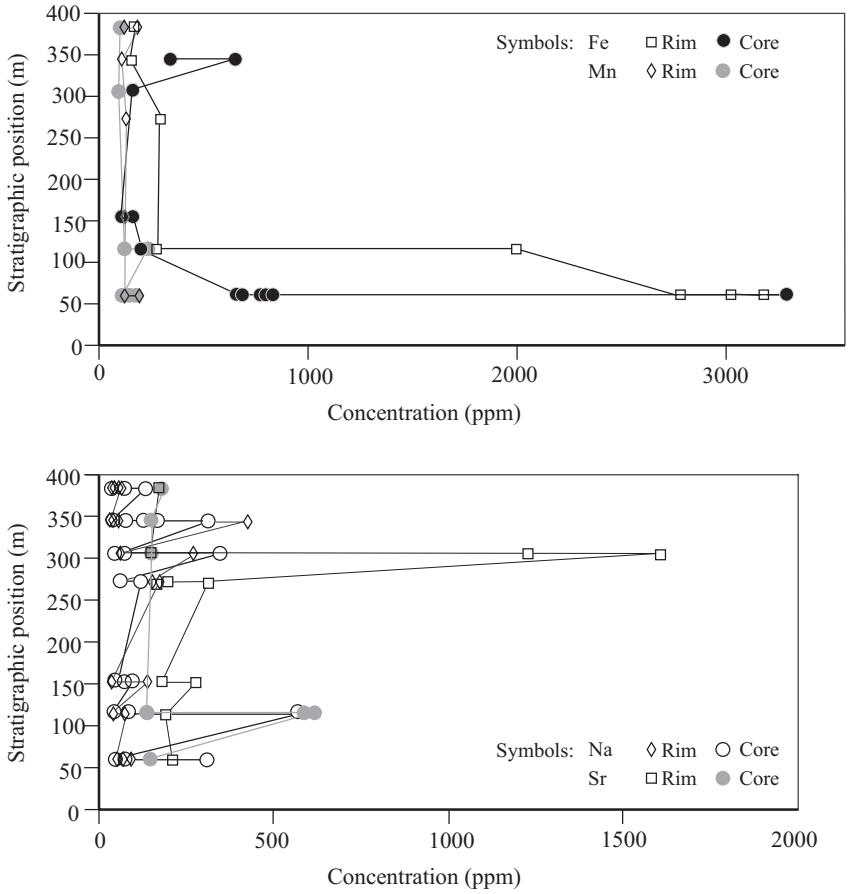

Figure 5. Trace element concentrations versus stratigraphic position in Cupido Formation carbonates from the Bustamante Canyon. In some cases, more than one analysis was performed for a stratigraphic positions. Overall, there are no obvious systematic patterns in the trace elements distribution in the Cupido Formation dolomites, although relatively high trace elements concentrations in some samples are noticed.

the strontium ratios of Late Cretaceous (Campanian) marine water (McArthur *et al.*, 2001). However, these more radiogenic ratios probably resulted from the interaction of the dolomitizing fluid with siliciclastic rocks, because it is unlikely that unmodified Late Cretaceous marine water have been the dolomitizing fluid, as is discussed below.

To aid with the genetic interpretation of the Cupido Formation dolomite, the $^{87}Sr/^{86}Sr$ ratios of eight samples from different components of the La Virgen Formation, which is the updip equivalent of the Cupido Formation, were also measured (Table 2). The La Virgen Formation is an inner platform, cyclic sedimentary succession consisting of shales, marine carbonates, and evaporites (Hernández Trejo, 2003). Since the La Virgen Formation has no age-diagnostic fossils its precise age is unknown. By stratigraphic position, its age could range from upper Hauterivian to the lower Aptian (Humphrey and Díaz, 1956; Alfonso-Zwanziger, 1978; Márquez-Domínguez, 1979; Charleston, 1981; Hernández-Trejo, 2003). The strontium isotopic ratios of two La Virgen gypsum samples are 0.70744 and 0.70748. These two values intersect the Sr-isotope curve of McArthur *et al.* (2001) at the Santonian-Campanian boundary and the Barremian. Likewise, two calcite samples from an oyster boundstone provided three strontium isotopic ratios of 0.70746, 0.70748 and 0.70757. The first two strontium ratios intersect the Sr-isotope curve of McArthur *et al.* (2001) at the Hauterivian, Barremian and Santonian; whereas the third one corresponds to Campanian sea water. Additionally, the strontium isotopic ratios measured for three samples of sabkha(?)-type dolomite were: 0.70748, 0.70757 and 0.70765, which are also similar to the strontium ratio of the Campanian sea water. These strontium isotopic ratios of La Virgen dolomites are very similar to those of the replacement dolomite of the Cupido Formation. Thus, it is very likely that the dolomitizing fluid of the Cupido Formation at Bustamante Canyon was influenced, in part, by more radiogenic fluids that interacted with siliciclastic sediments, coming from the most proximal updip inner platform area of the Cupido system.

Fluid inclusion analyses

In order to constrain the temperature conditions of the formation of the Cupido Formation dolomite, 98 fluid inclusion analyses were performed. These fluid inclusions

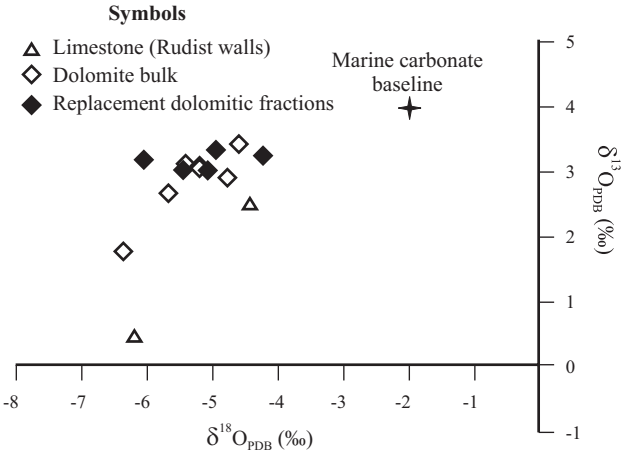

Figure 6. Carbon and oxygen isotopic composition of replacement dolomite and marine calcite from the Cupido Formation at Bustamante Canyon. The marine carbonate baseline value was estimated by Moldovanyi and Lohmann (1984) utilizing core samples from both Sligo and Cupido formations.

were present within both replacement dolomite and cement dolomite. Fluid inclusions in the Cupido Formation dolomite contain two phases (liquid-vapor) and their shape is rectangular or irregular. The fluid inclusions occur in both cores and rims of dolomite crystals (Figure 7). There are also fluid inclusions showing necking down and stretching that were not included in this study because they do not provide reliable dolomite formation temperatures (Crawford, 1981; Allan and Wiggins 1993; Martínez-Ibarra, 1999). Nearly 75% of the measured homogenization temperatures on the primary fluid inclusions in dolomites lie between 190 ºC and 200 ºC (Figure 8; Table 1). These homogenization temperature values strongly suggest that the dolomite in the Cupido Formation is a high-temperature diagenetic phase. Five measured homogenization temperatures range from 205 ºC to 217 ºC (Figure 8). The temperatures higher than 223 ºC are not considered as real homogenization temperatures; they are interpreted as the result of stretching probably due to post-dolomitization high temperatures. To evaluate if the high homogenization temperatures could extend southward of the Bustamante Canyon, 21 fluid inclusion analyses on both replacement and cement dolomites of the Cupido Formation from Potrero Minas Viejas and Potrero Chico (Figure 1) were performed in this investigation. The range of the homogenization temperatures in these southern localities spans also from 190 ºC to 200 ºC. Since large primary fluid inclusions are not common in the dolomite crystals, it was not possible to estimate melt temperatures. Therefore, it was unfeasible to infer the salinity of the diagenetic fluid that dolomitized the Cupido Formation at Bustamante Canyon.

Additionally, 32 measurements of homogenization temperatures on primary fluid inclusions of the post-dolomite calcite cement were performed. The obtained homogenization temperatures range from 170 ºC to 180 ºC for luminescent yellow bands and from 135 ºC to 145 ºC for non-luminescent and dull bands. These results are also indicative of high-temperature conditions. This suggests that the Cupido Formation remained deeply buried after the dolomitization process. For the fluid inclusions in the post-dolomite calcite cement, it was possible to infer the salinity of the diagenetic fluid utilizing three melt temperatures (Tm). These Tm are: -20.3 ºC, -8 ºC and -3.7 ºC, which correspond to salinities of 22.6 wt. %, 11.7 wt. % and 6.0 wt. % NaCl equivalents, respectively (Table 1). Thus, the fluid from which the post-dolomite calcite cement was precipitated probably was a hot brine**.**

POSSIBLE DOLOMITIZATION MECHANISMS OF THE CUPIDO FORMATION

The possible mechanisms that caused the high-temperature dolomitization of the Cupido Formation sedimentary succession at Bustamante Canyon are analyzed below.

Dolomite distribution

Murillo-Muñetón (1999) showed that the dolomite bodies within the Cupido Formation crosscut stratification planes. These stratigraphic relationships clearly imply a post-depositional origin for the dolomites. The Sierra de Bustamante is part of a NW-SE trending, large open anticline with no field evidence of major faulting (Figure 2). Only minor normal faults whose displacements are just a few meters are present in the area (Murillo-Muñetón, 1999). Thus, zones of intense deformation or fracturing are absent at Bustamante Canyon. It is clear that dolomite distribution is not spatially related to deformational features (*e.g.*, faulting or fractures zones). Rather, the geometries of massive dolomite bodies were controlled, in part, by facies types. For instance, the geometries of dolomite bodies are generally irregular in the lower part of the Cupido Formation, whose facies are mainly outer platform and platform margin facies.

Table 2. Strontium isotopic ratios of samples from the Lower Cretaceous La Virgen Formation.

Sample	Mineral	$^{87}Sr/^{86}Sr$	n	1 sd
V-1-A	calcite	0.70748	27	39
V-1-B	calcite	0.70746	58	34
V-36	calcite	0.70757	58	32
V-13-A	dolomite	0.70765	58	38
V-13-B	dolomite	0.70748	56	38
V-26	dolomite	0.70757	55	39
V-1	gypsum	0.70748	57	34
V-40	gypsum	0.70744	57	38

n: number of individual isotopic determinations; 1 sd: one standard deviation.

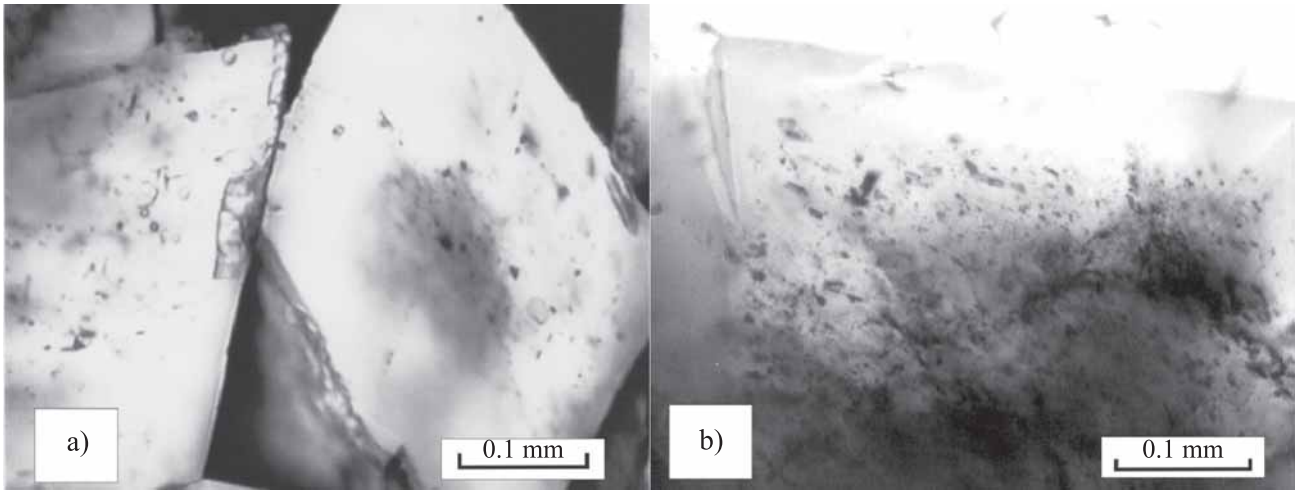

Figure 7. Photomicrographs of two-phase fluid inclusions in crystals of dolomite cement of the Cupido Formation. The fluid inclusions are located on both growth lines and crystal cores.

In contrast, the geometries of dolomite bodies are commonly tabular or subhorizontal in the upper part of the Cupido Formation whose facies are cyclic inner platform facies.

Diagenetic environment

Petrographic, microthermometric, and geochemical analyses of the carbonate phases strongly suggest that dolomitization of the Cupido Formation occurred in a deep-burial diagenetic environment. This interpretation is based on the following observations.

Shape of replacement dolomite crystals is mostly nonplanar forming mosaics of brownish anhedral crystals that commonly emulate the former crystal size of the dolomitized carbonate facies. Hence, lime mudstone facies were commonly transformed to fine-grained dolostones whereas coarser facies such as grainstone or packstone facies were transformed to coarse-grained dolostones. On the other hand, dolomite cement is commonly coarse grained and euhedral, and often present as the typical high-temperature saddle dolomite. These petrographic characteristics are diagnostic of deep-burial conditions (Radke and Mathis, 1980; Zenger, 1983; Morrow, 1990b; Tucker and Wright, 1990; Choquette and James, 1990; Purser *et al.*, 1994; Warren, 2000). Additional data that support this interpretation include (1) late diagenetic features such as mechanical compaction and pressure solution that pre-dates the dolomitization event and hydrocarbon migration, and (2) late high-temperature, blocky calcite cement that post-dates the massive dolomitization process. Dull red homogeneous luminescence also supports the interpretation that the dolomitization event of the Cupido Formation occurred under deep-burial conditions (Tucker and Wright, 1990). In contrast, the post-dolomite blocky calcite cement shows concentric zoning. The high concentrations of Fe (up to 3,292 ppm) also indicate deep-burial conditions for the formation of the dolomite (Dickson and Coleman, 1980; Reeder, 1981; Tucker and Wright, 1990; Allan and Wiggins, 1993; Warren, 2000).

The microthermometry of primary fluid inclusions of the Cupido Formation dolomites is one of the most striking supports for a deep-burial origin. The range of homogenization temperatures from primary fluid inclusions varies commonly from 190 ºC to 200 ºC and is considered as the minimum temperature range for the dolomite formation. It is likely that the dolomitization process could have reached maximum temperatures between 205 ºC and 217 ºC. This is suggested by fluid inclusion temperatures higher than 200 ºC reported for the Monterrey area by Gray *et al.* (2001) and Lefticariu *et al.* (2005). These temperature values are typical of a deep-burial diagenetic environment (Land, 1980; Zenger, 1983; Tucker and Wright, 1990; Allan and Wiggins 1993; Montañez, 1994; Qing and Mountjoy, 1994; Veizer, *et al.*, 1999; Warren, 2000). Moreover, fluid inclusions in the Cupido Formation dolomite are typically composed by two phases (liquid-vapor), which is a diagnostic characteristic of dolomite formed under high-temperature conditions in a deep-burial setting (Allan and Wiggins, 1993). The $\delta^{18}O_{PDB}$ values of the Cupido Formation replacement dolomites vary from -6.4 to -4.2‰ and unpublished oxygen isotopic data of replacement dolomite by G. Murillo-Muñetón range from -6.9 to -5.1‰. Those $\delta^{18}O_{PDB}$ values are relatively lighter than the $\delta^{18}O_{PDB}$ value (-2‰) estimated by Moldovanyi and Lohman (1984) for original marine carbonate composition for Lower Cretaceous time. Therefore, the relatively lighter $\delta^{18}O_{PDB}$ values of the Cupido Formation dolomites are interpreted to be the result of isotopic fractionation due to a thermal effect. On the other hand, the remarkably more negative $\delta^{18}O_{PDB}$ value of -10.2‰ for a sample of post-dolomite blocky calcite cement as well as the unpublished oxygen isotopic data by G. Murillo Muñetón are also inter-

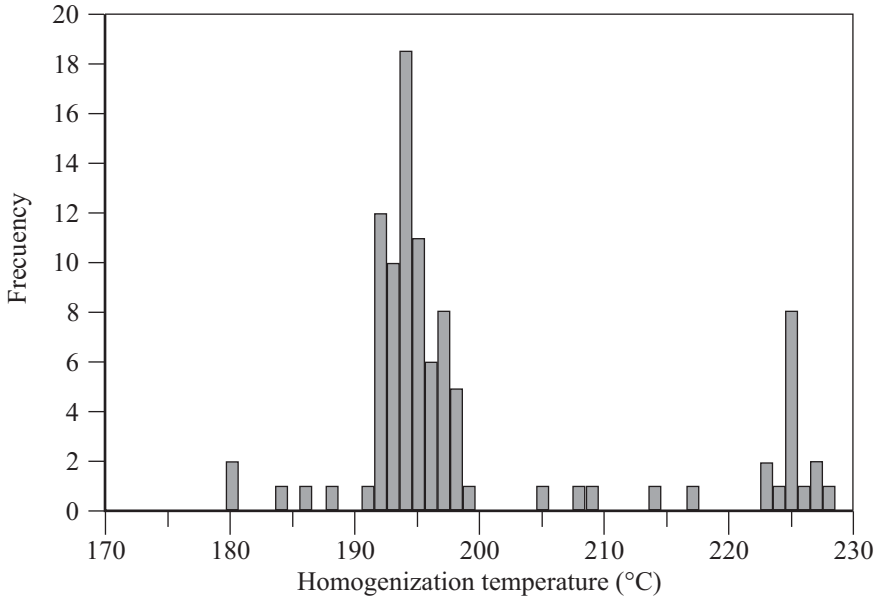

Figure 8. Histogram of homogenization temperatures measured in two-phase fluid inclusions in dolomite crystals from the Cupido Formation. Most of the measured temperatures lie between 190 ºC to 200 ºC; this temperature range is considered as the minimum temperature range for the dolomite formation in the Cupido Formation.

preted here as due to thermal effects. This indicates that the Cupido Formation continued under deep-burial conditions after the formation of the dolomite.

The $\delta^{18}O_{SMOW}$ value of the diagenetic fluid that dolomitized the Cupido Formation at Bustamante Canyon was calculated using the oxygen isotopic composition and homogenization temperatures of the dolomite. One geothermometric equation commonly used is the one of Friedman and O'Neil ($10^3 \ln\alpha_{dolomite\text{-}water} = 3.2 \times 10^6 T^{-2}$ (K) – 1.5; *e.g.*, Allan and Wiggins, 1991; Montañez, 1994). Considering that the homogenization temperatures range from 180 ºC to 200 ºC and the $\delta^{18}O_{PDB}$ values vary from -6.9 to -4.2‰, then the $\delta^{18}O_{SMOW}$ of the dolomitizing fluid ranges from +11 to +13‰. These calculations imply that the dolomitizing fluid was ^{18}O-enriched water compared to Cretaceous seawater whose $\delta^{18}O_{SMOW}$ was approximately -1‰ (Veizer *et al.*, 1999).

The Ca/Mg ratio of the Cupido Formation replacement dolomite ranges from 1.03 to 1.10 and indicates a nearly stoichiometric composition. The dolomite formed under high-temperature conditions tends to be more stoichiometric (Morrow, 1978, 1990a; Tucker and Wright, 1990). Stoichiometry may reflect a slow dolomite growth favored by the high-temperature regime (Morrow, 1978; Tucker and Wright, 1990; Barnaby and Read, 1992). Fabrics of dolomite including the common nonplanar mosaics of replacement dolomite and the saddle dolomite are a further support of late-stage diagenetic features under a high-temperature burial environment (Scoffin, 1987; Morse and Mackenzie, 1990; Tucker and Wright, 1990; Choquette and James, 1990; Barnaby and Read, 1992; Warren, 2000). The typical absence of crystal zoning observed in the scanning electron microscopy and cathodoluminescence studies of Cupido Formation dolomite suggest that the dolomitization most probably occurred as a single event rather than by steps. Absence of crystal zoning indicates that either the chemistry of the diagenetic fluid remained constant during the formation of the dolomite (Reeder, 1981; Tucker and Wright, 1990; Walker and Burley, 1991; Allan and Wiggins, 1993; Warren, 2000) or that no changes in the precipitation rate of the crystals occured (Tucker and Wright, 1990). According to those observations, the replacement dolomite apparently was not affected by significant recrystallization (Land, 1985; Kupecz *et al.*, 1993).

DISCUSSION

Probably, one of the most difficult tasks in carbonate diagenesis is deciphering the nature of the diagenetic fluids that dolomitize large masses of marine carbonates. In the case of the Cupido Formation dolomite, the chemical data do not unequivocally define the type of the dolomitizing fluid. However, stratigraphic information together with the collected geochemical data suggests that the diagenetic fluid of the Cupido Formation dolomite was perhaps formation water (modified sea water) from both the Cupido Formation and its updip equivalent La Virgen Formation. This inference is based on the spatial distribution of the dolomite and on the geometries of the dolomite bodies. The dolomite bodies occur only within the Cupido Formation and do not extend across the underlying Taraises Formation and the overlying La Peña Formation. Trace element concentrations of dolomite (111 to 3,292 ppm for Fe, 91 to 234 ppm

for Mn, 30 to 566 ppm for Na, and 131 to 1,608 ppm for Sr) fall within the range of formation water (Veizer, 1983; Morse and Mackenzie, 1990; Allan and Wiggins, 1993; Banner, 1995; Warren, 2000). The calculated $\delta^{18}O_{SMOW}$ of the dolomitizing fluid varying from +11 to +13‰ suggests ^{18}O-enriched water, probably saline water. $^{87}Sr/^{86}Sr$ ratios of the Cupido Formation dolomite are similar to those of the sabkha(?)-type dolomites of the La Virgen Formation. The $^{87}Sr/^{86}Sr$ ratios varying from 0.70754 to 0.70770 for Cupido Formation replacement dolomite and 0.70748 to 0.70765 for La Virgen Formation sabkha(?)-type dolomite, are slightly more radiogenic than the $^{87}Sr/^{86}Sr$ ratio (0.70749) of marine constituents of the Cupido Formation. As was mentioned above, the geometries of the dolomite bodies of the upper cyclic inner platform facies are in general tabular or subhorizontal. These observations suggest that formation water, slightly more radiogenic and probably more saline and with a higher Mg/Ca ratio, coming from La Virgen Formation moved basinward within the Cupido Formation facies and mixed with formation water of the Cupido Formation itself. Later, this diagenetic fluid partially dolomitized the calcareous facies of the Cupido Formation in a deep-burial, high-temperature environment.

Regarding the movement of the dolomitizing fluid and the pumping mechanism that allowed the dolomitization of the Cupido Formation at Bustamante Canyon, several inferences can be made consistent with the collected data. Field data indicate that the dolomitization process is restricted to the Cupido Formation and that it did not affected the underlying Taraises Formation and the overlying La Peña Formation. This fluid moved laterally along the beds of the Cupido Formation probably through the more porous and permeable beds. Both low-permeability units, the underlying Taraises Formation and overlying La Peña Formation, functioned as aquitards. This inference is compatible with the hydrologic system of passive margins proposed by Heydari (1997) that explain some dolomitization processes along the margins of the Gulf of Mexico Basin during Cretaceous time. It is very likely that the hydrologic mechanism could have been facilitated by convective thermohaline movements (Heydari, 1997) at the start of the Laramide Orogeny (Lawton and Giles, 1997).

The unusually high temperatures (190 ºC to 200 ºC) recorded in the dolomite of the Cupido Formation at Bustamante Canyon are higher than the expected temperatures for a tectonic passive margin (*e.g.*, from 50 ºC to 100 ºC; Warren, 2000). The typical geothermal gradient in this type of tectonic scenario varies from 15 ºC/km to 30 ºC/km (Warren, 2000). Considering that the maximum burial depth reached by the Cupido Formation in this tectonic scenario (*e.g.*, a passive margin) was roughly 5 km (Goldhammer *et al.*, 1991), the maximum value for the geothermal regime (30 ºC/km), and an assumed surface temperature of 20 ºC then the maximum expected temperature would be 170 ºC. If we consider an average geothermal regime (20 ºC/km) and the same maximum burial depth and assumed surface temperature, then the maximum expected temperature would only be 120 ºC. These hypothetical temperature values are lower than the temperatures documented in this study, therefore, it is likely that a thermal anomaly was the cause of the extra heat recorded in the Cupido Formation dolomite and the post-dolomite calcite cement. The thermometric data from this work and the study of Gray *et al.* (2001) suggest that this thermal anomaly was regionally extensive. Gray *et al.* (2001) carried out an integrated regional study to define the thermal evolution of the Sierra Madre Oriental fold belt utilizing fluid inclusion analysis and geochronological techniques. These authors reported homogenization temperatures for the Monterrey salient area from 140 ºC to 240 ºC, with most temperatures varying from 150 ºC to 200 ºC. The high temperatures measuredin this work, 190 ºC to 200 ºC, also in Cupido Formation dolomites from Potrero Minas Viejas and Potrero Chico, located approximately 65 and 70 km southward, respectively, support the presence of that thermal anomaly. This conclusion is also supported by thermometric work, based on fluid inclusions, conducted in the area of Monterrey by Lefticariu *et al.* (2005). These authors determined homogenization temperatures from 180 ºC to 220 ºC for calcite cements of the Cupido Formation.

The origin of the documented regional thermal anomaly is not fully understood. This thermal anomaly could have originated by either regional magmatism or halokinetic activity. Damon and Clark (1981) estimated that the magmatic arc developed during Late Cretaceous and early Tertiary times and associated with the Laramide Orogeny (between 80 and 60 My ago) along the Pacific margin, extended for 700 km into the hinterland region. However, the studied area was located at least 900 km away from the Pacific trench, and it could not have been affected by the magmatic activity related to the Laramide Orogeny. Indeed, there are no reports of Late Cretaceous-early Tertiary plutons in the Monterrey-Bustamante corridor. The magmatic bodies cropping out about 13 km northeast of Bustamante Canyon near Candela, State of Coahuila, consist of small granitic stocks, that developed contact metamorphic aureoles affecting the Cretaceous marine sediments. K-Ar ages of 44.29 ± 0.19 Ma (hornblende) and 41.23 ± 0.02 Ma (biotite) reported by Chávez-Cabello *et al.* (2002) for these magmatic bodies suggest that these plutons are post-Laramide in age (Middle Eocene). As was cited above, the Laramide Orogeny deformed the Cupido Formation after the high-temperature dolomitization event, hence, the Middle Eocene magmatic event obviously was not responsible for the regional thermal anomaly.

An alternative origin for the regional thermal anomaly implies saline structures (Warren, 2000). The salt bodies conduct heat more efficiently than common sedimentary rocks such as shale, sandstone, and limestone (O'Brien and Lerche, 1987). Besides, the massive salt structures have a more extensive vertical relief providing high conductivity pathways for heat coming up from deeper beds (O'Brien and Lerche, 1987). The thick Minas Viejas Formation,

dominated by marine halite and gypsum, is widely distributed throughout northeastern Mexico and salt diapirs are well documented in this region (Weidie and Murray, 1967; Weidie and Wolleben, 1969; McBride *et al.*, 1974; Laudon, 1984; Giles and Lawton, 2002). Using a geothermal gradient of 30 ºC/km and assuming a surface temperature of 10 ºC, Millán-Garrido (2004) calculated paleotemperatures suggesting that, by the time of deformation, the top of the Minas Viejas salt horizon had temperatures between >150 ºC and 197 ºC in the La Popa Basin. Although, it is not well known when the diapiric activity began in northeastern Mexico, it is likely that this halokinetic activity started during the onset of the tectonic compressive event related to the Laramide Orogeny in Maastrichtian time (Millán-Garrido, 2004). Detailed stratigraphic analysis of the Papalote diapir area in the La Popa Basin demonstrated that the salt movement was active during the deposition of late Maastrichtian-Early Paleocene siliciclastic and carbonate sediments (Giles and Lawton, 2002).

Gray *et al.* (2001) concluded that a foreland basin was developed contemporaneously and adjacent to the Sierra Madre Oriental fold belt during the Laramide Orogeny. That foreland basin included the Parras and La Popa basins and probably extended northward into the Sabinas Basin (Gray *et al.*, 2001). These authors documented temperatures between 140 ºC to 155 ºC in the La Popa Basin. As was pointed out previously, they also reported high homogenization temperatures varying from 140 ºC to 250 ºC, ranging the majority from 150 ºC to 200 ºC, for Upper Jurassic to Eocene samples from the Monterrey salient area. Gray *et al.* (2001) interpreted their measured high temperatures as the result of normal burial assuming a geothermal gradient of 30 ºC/km in a foreland tectonic setting. Hence, the La Popa Basin was buried from 5 to 6 km (Gray *et al.*, 2001). To explain the unusual higher temperatures for the Monterrey salient area, they proposed that this region (part of the Parras Basin) reached a deeper burial depth, probably of 7 km. Recently, Gray *et al.* (2005) also documented relatively high temperatures of 150 ºC for Cretaceous sediments from the Sabinas Basin and also attributed them to normal burial conditions. If the Bustamante Canyon area was part of the same tectonic scenario as that proposed for the Monterrey region, which was buried up to 7 km in a foreland setting, it would explain the similar high temperatures measured in the Cupido Formation dolomite. However, the Bustamante Canyon area was located approximately in the northeastern part of the La Popa foreland basin, where the basin was relatively thinner. Therefore, we would expect lower temperatures than those measured in the Cupido Formation dolomite. If the actual burial depth reached at Bustamante Canyon could be estimated and the accurate timing of the dolomitization event could be constrained (see below), then it would be possible to evaluate whether the cause of the thermal anomaly was solely normal burial.

Defining unequivocally the timing of the dolomitization event of the Cupido Formation is also difficult. There is some tectonic information that suggests that the Cupido Formation was dolomitized perhaps during Late Cretaceous time. The fact that the dolomite distribution is not spatially related to major tectonic features such as faults or fractures implies that the dolomite was formed before significant tectonic deformation. This is consistent with one of the main conclusions of this work, that is, the dolomite was formed under a deep-burial diagenetic environment. Furthermore, the superb Cupido Formation outcrops at Bustamante Canyon clearly show that the dolomitized bodies, mainly the tabular-shaped bodies in the upper cyclic inner platform facies, are also folded as are the undolomitized limestone beds. Regarding the post-dolomite calcite cement, its cathodoluminescence patterns (zoning), homogenization temperatures (135 ºC to 180 ºC), $\delta^{18}O_{PDB}$ values (-10.2‰) and trace element concentrations (207 to 3,148 ppm for Fe, 91 to 234 ppm for Mn, 56 to 616 ppm for Na, and 134 to 789 ppm for Sr) considered together are diagnostic also of deep-burial diagenetic conditions (Morrow, 1990a; Tucker and Wright, 1990; Allan and Wiggins, 1993). This information also implies that the Cupido Formation probably still remained deeply buried after the dolomitization event. Moreover, both thermometric data of the post-dolomite calcite cement and the interpreted stretching in the fluid inclusions of dolomite also suggest that the regional thermal anomaly persisted after the dolomitization process of the Cupido Formation. Thus, the dolomitization of the Cupido Formation at Bustamante Canyon occurred perhaps during the initial stage of the Laramide Orogeny, which took place from Late Cretaceous to Eocene time (Lawton and Giles, 1997) and also probably caused the onset of the main saline diapiric activity in the region.

CONCLUSIONS

The main conclusions of this study are as follows.

1. The Lower Cretaceous Cupido Formation is partially dolomitized at Bustamante Canyon. The dolomite distribution is complex, forming massive irregular to tabular/subhorizontal bodies not spatially related to major tectonic deformation (faults or fractures). Dolomite distribution crosscuts bedding planes throughout the Cupido Formation. Geometries of dolomite bodies in the lower part of the Cupido Formation, dominated by platform margin and outer platform facies, are irregular masses. In contrast, geometries of dolomite bodies in the upper part of the Cupido Formation, dominated by cyclic inner platform facies, are tabular to subhorizontal.

2. The Cupido Formation dolomite is dark gray in color and consists mostly of replacement dolomite and minor dolomite cement. Crystal size of dolomite was controlled, in part, by the former depositional fabrics of the calcareous facies. Fine-grained dolomite occurs mainly in carbonate mud-rich facies and coarser dolomite is found mostly in carbonate mud-poor lithofacies. Both replacement

dolomite and dolomite cement show dull luminescence with a typical homogeneous red color, lacking zoning. In contrast, post-dolomite blocky calcite cement shows concentric zoning consisting of alternating brilliant bands, dull bands and non-luminescent bands.

3. Plane light petrography, cathodoluminescence and epifluorescence petrography, trace element geochemistry, oxygen stable isotopes and fluid inclusion microthermometry indicate unquestionably that the formation of the Cupido Formation dolomite occurred in a deep-burial diagenetic environment. Unexpectedly high homogenization temperatures, ranging from 190 ºC to 200 ºC, measured from two-phase fluid inclusions in replacement dolomite allow defining the Cupido Formation dolomite as a high-temperature diagenetic phase.

4. Strontium isotopic ratios from the Cupido Formation carbonate phases (calcite and dolomite) suggest that the dolomitizing fluid was slightly more radiogenic water (modified sea water) rather than solely formation water of the Cupido Formation. Strontium isotopic ratios from carbonate phases and evaporites from the inner platform La Virgen Formation, an updip Cupido Formation equivalent, and the fact that the underlying Taraises Formation and the overlying La Peña Formation are undolomitized, suggest that the dolomitizing fluid was perhaps a mixture of saline brines coming laterally from the Virgen Formation that mixed eventually with formation water (modified sea water) of the Cupido Formation itself. This dolomitizing fluid was heated up by a high-temperature regime that facilitated the dolomitizing pumping mechanism and the dolomitization process as well.

5. The unusually high temperatures (190 ºC to 200 ºC) recorded in the two-phase fluid inclusions of the Cupido Formation replacement dolomite from Bustamante Canyon and other southern locations (Potrero Minas Viejas and Potrero Chico) are higher than the temperatures (50 ºC to 100 ºC) that would be expected in a typical passive margin tectonic setting. It is proposed that a regional thermal anomaly existed in the study area during the time of the formation of the Cupido Formation dolomite. The origin of this thermal anomaly is not fully understood; it is likely the result of halokinetic activity which has been well documented in northeast Mexico. Salt structures of the Jurassic Minas Viejas Formation acted perhaps as efficient conduits of heat coming up from deeper beds. Although similar and/or higher temperatures for the Monterrey salient area are known and attributed by previous studies to deep-burial conditions in a foreland setting, more geologic data are needed to evaluate whether this interpretation also applies to the Cupido Formation dolomite at Bustamante Canyon.

6. Timing of the dolomitization event of the Cupido Formation is still unknown. However, field relationships suggest that the dolomitization process took place probably during Late Cretaceous time at the start of the Laramide Orogeny. There is no spatial relation of dolomite bodies to major tectonic features (*e.g.*, faults or fractures) implying that the dolomite was formed before significant tectonic folding. The presence of post-dolomite calcite cement that also represents a deep-burial diagenetic phase indicates that the Cupido Formation remained buried deeply after the dolomitization event.

ACKNOWLEDGEMENTS

This study was financially supported by the Fondo para la Investigación con Instituciones de Educación Superior from the Instituto Mexicano del Petróleo (IMP). It was part of the research project FIES-98-76-1. Further financial support for the oxygen and carbon stable isotope analyses was provided by CONACYT (Project G35442-T). We thank the authorities from the IMP, Universidad Nacional Autónoma de México (Instituto de Geología and Instituto de Geofísica), and CONACYT for the financial support and utilization of their facilities. This work represents the results of the senior author's master thesis. This paper was significantly improved by the constructive reviews of Eugene Perry (Northern Illinois University) and Gary C. Gray (ExxonMobil Upstream Research Company). Dr. Arturo Martín also provided important observations on the manuscript. Martín Hernández Trejo supplied samples of the La Virgen Formation. We also are grateful to Gabriela Solís, Edith Cienfuegos, Pedro Morales, Elena Lounejeva, Rosalinda Rodríguez, and Rufino Lozano for their assistance in the analytical work.

REFERENCES

Alfonso-Zwanziger, J., 1978, Geología regional del sistema sedimentario Cupido: Boletín de la Asociación Mexicana de Geólogos Petroleros, 30, 1-55.

Allan, J.R., Wiggins, W.D., 1993, Dolomite Reservoirs: American Association of Petroleum Geologists, Curse Note Series # 36, 129 p.

Banner, J.L., 1995, Application of the trace element and isotope geochemistry of strontium to studies of carbonate diagenesis: Sedimentology, 45(2), 805-824.

Barnaby, G.J., Read, J.F., 1992, Dolomitization of a carbonate platform during late burial: Lower to Middle Cambrian shady dolomite, Virginia Appalachians: Journal of Sedimentary Petrology, 62(6), 1023-1043.

Carrillo-Bravo, J., 1961, Geología del Anticlinorio Huizachal-Peregrina al N-W de Ciudad Victoria, Tamaulipas: Boletín de la Asociación Mexicana de Geólogos Petroleros, 13, 1-98.

Charleston, S., 1973, Stratigraphy, tectonics, and hydrocarbon potential of the Lower Cretaceous, Coahuila Series, Coahuila, Mexico: The University of Michigan, Ph. D. Dissertation, 268 p. (unpublished).

Charleston, S., 1981, A summary of the structural geology and tectonics of the state of Coahuila, Mexico, *in* Smith, C.I. (eds.), Lower Cretaceous Stratigraphy and Structure, Northern Mexico: West Texas Geological Society, Publication 81-74, 28-36.

Chávez-Cabello, G., Aranda-Gómez, J.J., Tovar-Cortés, J A., Morton-Bermea, O.E Iriondo, A., 2002, Relación entre la deformación compresiva y la actividad magmática del paleógeno en el Cinturón Plegado de Coahuila, México, *in* XII Congreso Nacional de Geoquímica, Puerto Vallarta, Jal.: Instituto Nacional

de Geoquímica, Actas INAGEQ, 8(1), 167-168.

Choquette, P.W., James, N.P., 1990, Limestone –the burial diagenetic environment, *in* McIlreath, I.A., and Morrow, D.W. (eds.), Diagenesis: Ottawa, The Runge Press Ltd., Geoscience Canada, Reprint Series 4, 75-111.

Conklin, J., Moore, C., 1977, Paleoenvironmental analysis of the Lower Cretaceous Cupido Formation, northeast Mexico, in Bebout, D.G., Loucks, R.D. (eds.), Cretaceous Carbonates of Texas and Mexico Applications of Subsurface Exploration: The University of Texas at Austin, Bureau of Economic Geology, Report of Investigations, 89, 302-323.

Crawford, M.L., 1981, Phase equilibria in aqueous fluid inclusions, *in* Hollister, L.S., Crawford M.L. (eds.), Short Course in Fluid Inclusions. Applications to Petrology: Mineralogical Association of Canada, Short Course Handbook 6, 75-100.

Damon, P.E., Clark, K.F., 1981, Evolución de los arcos magmáticos en México y su relación con la metalogénesis: Universidad Nacional Autónoma de México, Revista del Instituto de Geología, 5, 1981 (1984), 223-238.

Dickson, J.A.D., 1966, Carbonate identification and genesis as revealed by staining: Journal of Sedimentary Petrology, 36, 491-505.

Dickson, J.A.D., Coleman, M.L., 1980, Changes in carbon and oxygen isotope composition during limestone diagenesis: Sedimentology, 27, 107-118.

García, A., Gallo, I., Aguilera, L., 1989, Interpretación geológica regional en el Prospecto Magiscatzin I, N. L., Tamps.: Instituto Mexicano del Petróleo, Subdirección de Tecnología de Exploración, Proyecto C-4013, 182 p. (unpublished).

Giles, K.A., Lawton, T.F., 2002, Halokinetic sequence stratigraphy adjacent to the El Papalote diapir, northeastern México: American Association of Petroleum Geologists Bulletin, 86(5), 823-840.

Goldhammer, R.K., 1995, Geologic field log for Mesozoic of the Sierra Madre Oriental in the Monterrey-Saltillo salient: American Association of Petroleum Geologists, Field Trip # 10, 18 p.

Goldhammer, R.K., 1999, Mesozoic sequence stratigraphy and paleogeographic evolution of northeast Mexico, *in* Bartolini, C., Wilson, J.L., Lawton, T.F. (eds.), Mesozoic Sedimentary and Tectonic History of North-Central Mexico: Geological Society of America, Special Paper 340, 1-58.

Goldhammer, R.K., Lehmann, P.J., Todd, R.G., Wilson, J.L., Ward, W.C., Johnson, C.R., 1991, Sequence Stratigraphy and Cyclostratigraphy of the Mesozoic of the Sierra Madre Oriental, Northeast Mexico, a Field Guidebook: Gulf Coast Section Society of Economic Paleontologists and Mineralogists, 85 p.

Gray, G., Pottorf, R.J., Lopez, C.J., Atkinson, G.L., 2005, Maduración termal y levantamiento regional del noreste de México (abstract in CD-ROM), *in* Simposium sobre Plays y Yacimientos de Aceite y Gas en Rocas Siliciclásticas, Reynosa, Mexico: Asociación Mexicana de Geólogos Petroleros, Resúmenes, CD-ROM.

Gray, G.G., Pottorf, R.J., Yurewicz, D.A., Mahon, K.I., Pevear D.R., Chuchla, R.J., 2001, Thermal and chronological record of syn- and post-Laramide burial and exhumation, Sierra Madre Oriental, Mexico, *in* Bartolini, C., Buffler, R.T., Cantú-Chapa, A. (eds.), The Western Gulf of Mexico Basin: Tectonics, Sedimentary Basins, and Petroleum Systems: American Association of Petroleum Geologists, Memoir 75, 159-181.

Guzmán, A.E., 1974, Diagénesis de la Caliza Cupido del Cretácico Inferior, Coahuila, México: Revista del Instituto Mexicano del Petróleo, 6, 20-40.

Guzmán-García, J., 1991, Evaluación geológica petrolera del Golfo de Sabinas: Petróleos Mexicanos, Informe Técnico NE-M 2362, 72 p. (unpublished).

Heydari, E., 1997, The role of burial diagenesis in hydrocarbon destruction and H_2S accumulation, Upper Jurassic Smackover Formation, Black Creek Field, Mississippi: American Association of Petroleum Geologists Bulletin, 81(1), 26-45.

Hernández Trejo, J.M., 2003, Cicloestratigrafía en un sistema carbonatado-evaporítico del Cretácico Inferior, Formación La Virgen, noreste de México: Instituto Politécnico Nacional, Escuela Superior de Ingeniería y Arquitectura, Unidad Ticomán, Master Thesis, 86 p. (unpublished).

Hudson, J.D., 1977, Stable isotopes and limestone lithification: Journal of the Geological Society of London, 133, 637-660.

Humphrey, W.E., 1949, Geology of the Sierra de Los Muertos area, Mexico (with descriptions of Aptian cephalopods from the La Peña Formation): Geological Society of America Bulletin, 6, 89-176.

Humphrey, W.E., Díaz, G.T., 1956, Jurassic and Lower Cretaceous stratigraphy and tectonics of northeast Mexico: Petróleos Mexicanos, Informe Técnico NE-M 799, 393 p. (unpublished)

Imlay, R.W., 1936, Geology of the western part of the Sierra de Parras, Coahuila, Mexico: Geological Society of America Bulletin, 47, 1091-1152.

International Commision on Stratigraphy, 2004, International Stratigraphic Chart (on line): International Union of Geological Sciences, International Commision on Stratigraphy, <http://www.stratigraphy.org/chus.pdf>

Kellum, L.B., Imlay, R.W., Kane, W.G., 1936, Evolution of the Coahuila Peninsula, Mexico, Part I. Relation of structure, stratigraphy, and igneous activity to an early continental margin: Geological Society of America Bulletin, 47, 969-1008.

Kupecz, J.A., Montañez, I.P., Gao, G., 1993, Recrystallization of dolomite with time, *in* Rezak, R., Lavoie, D.L. (eds.), Carbonate Microfabrics: New York, Springer-Verlag, Frontiers in Sedimentary Geology, 187-194.

Land, L.S., 1980, The isotopic and trace element geochemistry of dolomite: the state of the art, *in* Zenger, D.H. Dunham, J.B., Ethington, R.L. (eds.), Concepts and Models of Dolomitization: Society of Economic Paleontologists and Mineralogists, Special Publication 28, 87-110.

Land, L.S., 1985, The origin of massive dolomite: Journal of Geological Education, 33, 112-125.

Laudon, R.C., 1984, Evaporite diapirs in the La Popa basin, Nuevo Leon, Mexico: Geological Society of America Bulletin., 95, 1219-1225.

Lawton, T.F., Giles, K.A., 1997, El Papalote Diapir, La Popa Basin: structure, stratigraphy and paleontology of Late Cretaceous-Early Tertiary Parras-La Popa near Foreland Basin near Monterrey, northeast Mexico, Tulsa, Oklahoma: American Association of Petroleum Geologists, Field Trip Guidebook 10, 55-74.

Lefticariu, L., Perry, E.C., Fisher, M.P., Banner, J.L., 2005, Evolution of fluid compartmentalization in detachment fold complex: Geology, 33(1), 69-72.

Lehmann, C., Osleger, D.A., Montañez, I.P., 1998, Controls on cyclostratigraphy of Lower Cretaceous carbonates and evaporites, Cupido and Coahuila platforms, northeastern Mexico: Journal of Sedimentary Research, 68, 1109-1130.

Lehmann, C., Osleger, D.A., Montañez, I.P., 1999, Evolution of Cupido and Coahuila carbonate platforms, Early Cretaceous, northeastern Mexico: Geological Society of America Bulletin, 111(7), 1010-1029.

Lehmann, C., Osleger, D.A., Montañez, I.P., 2000, Sequence stratigraphy of Lower Cretaceous (Barremian-Aptian) carbonate platforms of northeastern Mexico: regional and global correlations: Journal of Sedimentary Research, 70, 373-391.

Lohmann, K.C., 1988, Geochemical patterns of meteoric diagenetic systems and their application to studies of paleokarst, *in* James, N.P., Choquette, P.W. (eds.), Paleokarst: New York, Springer-Verlag, 58-80.

Márquez-Domínguez, B., 1979, Proyecto Formación La Virgen (Parámetros que controlan la producción en La Virgen): México, D.F., Petróleos Mexicanos, Informe Técnico NE-M-1594, 49 p.

Martínez-Ibarra, R., 1999, Estudio de inclusiones fluidas en dolomita asociados a emplazamiento de hidrocarburos: Parte sur del Campo Cantarell, Zona Marina-Campeche: México, Universidad Nacional Autónoma de México, Master Thesis, 90 p. (unpublished).

McArthur, J.M., Howarth, R.J., Bailey, T.R., 2001, Strontium isotope stratigraphy: LOWESS version 3. Best-fit line to the marine Sr isotope curve for 0 to 509 Ma and accompanying look up table for deriving numerical age: Journal of Geology, 109, 155-169.

McBride, E.F., Weidie, A.E., Wolleben, J.A., Laudon, R.C., 1974,

Stratigraphy and structure of the Parras and La Popa basins, northeastern Mexico: Geological Society of America Bulletin, 84, 1603-1622.

McFarlan, E. Jr., Menes, L.S., 1991, Lower Cretaceous, *in* Salvador, A. (ed.), The Gulf of Mexico Basin: Geological Society of America, The Geology of North America, J, 181-204.

Michalzik, D., 1991, Facies sequence of Triassic-Jurassic red beds in the Sierra Madre Oriental (NE Mexico) and its relation to the early opening of the Gulf of Mexico: Sedimentary Geology, 71, 243-259.

Millán-Garrido, H., 2004, Geometry and kinematics of compressional growth structures and diapirs in the La Popa basin of northeast Mexico: Insights from sequential restoration of a regional cross section and three-dimensional analysis: Tectonics, 23, 1-21.

Moldovanyi, E.P., Lohmann, K.C., 1984, Isotopic and petrographic record of phreatic diagenesis: Sligo and Cupido formations: Journal of Sedimentary Petrology, 54, 972-985.

Montañez, I.P., 1994, Late diagenetic dolomitization of Lower Ordovician, Upper Knox carbonates: a record of the hydrodynamic evolution of the southern Appalachian Basin: American Association of Petroleum Geologists Bulletin, 74(8), 1210-1239.

Morse, J.W., Mackenzie, F.T., 1990, Geochemistry of Sedimentary Carbonates: The Netherlands, Elsevier Science Publishers B.V., Developments in Sedimentology 48, 707 p.

Morrow, D.W., 1978, The influence of the Mg/Ca ratio and salinity on dolomitization in evaporite basins: Bulletin of Canadian Petroleum Geology, 26, 389-392.

Morrow, D.W., 1990a, Dolomite –Part 1: The Chemistry of Dolomitization and Dolomite Precipitation, *in* McIlreath, I.A., Morrow, D.W. (eds.), Diagenesis: Ottawa, The Runge Press Ltd., Geoscience Canada, Reprint Series 4, 113-123.

Morrow, D.W., 1990b, Dolomite –Part 2: Dolomitization Models and Ancient Dolostones, *in* McIlreath, I.A., Morrow, D.W. (eds.), Diagenesis: Ottawa, The Runge Press Ltd., Geoscience Canada, Reprint Series 4, 125-139.

Murillo-Muñetón, G., 1999, Stratigraphic architecture, platform evolution, and mud-mound development in the Lower Cupido Formation (Lower Cretaceous), northeastern Mexico: Texas, U.S.A., Texas A & M University, Ph. D. Dissertation, 153 p. (unpublished)

Murillo-Muñetón, G., Dorobek, S.L., 2003, Control on the evolution of carbonate mud mounds in the Lower Cretaceous Cupido Formation, northeastern Mexico: Journal of Sedimentary Research, 73(6), 869-886.

O'Brien, J.J., Lerche, I., 1987, Heat flow and thermal maturation near salt diapers, *in* Lerche, I., O'Brien, J.J. (eds.), Dynamical Geology of Salt and Related Structures: San Diego, Academic Press, 711-751.

Qing, H., Mountjoy, E.W., 1994, Formation of coarsely crystalline, hydrothermal dolomite reservoirs in the Prequ'ile Barrier, western Canada sedimentary Basin: American Association of Petroleum Geologists Bulletin, 78(1), 55-77.

Padilla y Sánchez, R.J., 1978, Geología y estratigrafía (Cretácico Superior) del límite suroeste del estado de Nuevo León: Universidad Nacional Autónoma de México, Revista del Instituto de Geología, 2(1), 37-44.

Purser, B.H., Tucker, M.E., Zenger, D.H., 1994, Problems, progress, and future research concerning dolomites and dolomitization, *in* Purser, B., Tucker, M., Zenger, D. (eds.), Dolomites, a Volume in Honor of Dolomieu: Oxford, Blackwell Scientific Publications, International Association of Sedimentologists, Special Publication 21, 3- 20.

Radke, R.M., Mathis, R.L., 1980, On the formation and occurrence of saddle dolomite: Journal of Sedimentary Petrology, 50, 1149-1168.

Reeder, R.E., 1981, Electron optical investigation of sedimentary dolomites: Contributions to Mineralogy and Petrology, 76, 148-157.

Revez, K.R., Landwehr, J.M., 2002, $\delta^{13}C$ and $\delta^{18}O$ isotopic composition of $CaCO_3$ measured by continuous flow isotope ratio mass spectrometry statistical evaluation and verification by application to Devils Hole Core DH-11 calcite: Rapid Communications in Mass Spectrometry 16, 2102-2114.

Revez, K.R., Landwehr, J.M., Keybl, J., 2001, Measurement of $\delta^{13}C$ and $\delta^{18}O$ isotopic ratios of $CaCO_3$ using a thermoquest Finnigan Gas Bench II Delta Plus XL Continuous flow isotope ratio mass spectrometer with application to Devils Hole Core DH-11 calcite: United States Geological Survey, Open-File Report 01-257.

Salvador, A., 1987, Late Triassic-Jurassic paleogeography and origin of Gulf of Mexico Basin: American Association of Petroleum Geologists Bulletin, 71, 419-451.

Scoffin, T.P., 1987, An Introduction to Carbonate Sediments and Rocks: Bishopgriggs, Blackie & Son Ltd, 274 p.

Selvius, D.B., Wilson, J.L., 1985, Lithostratigraphy and algal-foraminiferal biostratigraphy of the Cupido Formation, Lower Cretaceous, northeast Mexico, *in* Perkins, B.F., Martin, G.B. (eds.), Habitat of Oil and Gas in the Gulf Coast: Society of Economic Paleontologists and Mineralogists, Gulf Coast Section, Proceedings of the Fourth Annual Research Conference, 285-311.

Sibley, D.F., Gregg, J.M., 1987, Classification of dolomite rock textures: Journal of Sedimentary Petrology, 57(6), 967-975.

Tucker, M.E., Wright, V.P., 1990, Carbonate Sedimentology: Oxford, Blackwell Scientific Publications, 482 p.

Veizer, J., 1983, Chemical diagenesis of carbonates: theory and application of trace element technique, *in* Arthur, M.A. Anderson, T.F. (eds.), Stable Isotopes in Sedimentary Geology: Society of Economic Paleontologists and Mineralogists, Short Course 10, 3.1- 3.100.

Veizer, J., Ala, D., Bruckschen, P., Buhl, D., Bruhn, F., Carden, G.A.F., Diener, A., Ebneth, S., Godderis, Y., Jasper, T., Korte, C., Pawellek, F., Podlaba, O.G, Strauss, H., 1999, $^{87}Sr/^{86}Sr$, $\delta^{13}C$ and $\delta^{18}O$ evolution of Phanerozoic seawater: Chemical Geology, 161, 59-88.

Walker, G., Burley, S.D., 1991, Luminescence petrography and spectroscopic studies of diagenetic minerals, i*n* Barker, C.E., Koop, O. (eds.), Luminescence Microscopy: Quantitative and Qualitative Aspects: Society of Economic Paleontologists and Mineralogists, Short Course Notes 11, 83-96.

Warren, J.K., 2000, Dolomite: occurrence, evolution and economically important associations: Earth-Science Reviews, 52, 1-81.

Weidie, A.E., Murray, G.E., 1967; Geology of the Parras Basin and adjacent areas of northeastern Mexico: American Association of Petroleum Geologists Bulletin, 51, 678-695.

Weidie, A.E., Wolleben, J.A., 1969, Upper Jurassic stratigraphic relations near Monterrey, Nuevo León, Mexico: American Association of Petroleum Geologists Bulletin, 53(12), 2418-2420.

Wilson, J.L., 1990, Basement structural controls on Mesozoic carbonate facies in northeastern Mexico -a review, *in* Tucker, M.E., Wilson, J.L Crevello, P.D. Sarg, J.R., Read, F.R. (eds.), Carbonate Platforms Facies, Sequences and Evolution: Oxford, Blackwell Scientific Publications, International Association of Sedimentologists, Special Publication 9, 235- 255.

Wilson, J.L., Ward, W.C., Finneran, J., 1984, A Field Guide to Upper Jurassic and Lower Cretaceous Carbonate Platform and Basin Systems Monterrey-Saltillo Area, Northeast Mexico: Society of Economic Paleontologists and Mineralogists, Gulf Coast Section, 76 p.

Zárate-Mendoza, J.P., 1984, Evaluación geológica-económica del Golfo de Sabinas I, Prospecto: Cretácico Inferior (Neocomiano) Sabinas I: Petróleos Mexicanos (PEMEX), Informe Técnico NE-M-1965, 71 p. (unpublished).

Zenger, D.H., 1983, Burial dolomitization in the lost Burro Formation (Devonian), east-central California, and the significance of late diagenetic dolomitization: Geology, 11, 519-522.

Manuscritpt received: June 2, 2006
Corrected manuscript received: September 6, 2006
Manuscript accepted: December 4, 2006